Kondo and anti-Kondo coupling to local moments in EuB_6

J. Kunes[1,2] and W. E. Pickett[1]

[1]Department of Physics, University of California, Davis CA 95616, USA
[2]Institute of Physics, AS CR, Cukrovarnicka 10, 162 58 Praha 6, Czech Republic

(Dated: April 14, 2024)

With a treatment of the 4f states of EuB_6 based on LDA+U method, the mixing of Eu f states with B p states around the X point of the Brillouin zone is shown to have unexpected consequences for the effective exchange interactions. We analyze in detail the orbital character of electronic states close to the Fermi level and discuss the effective exchange between the itinerant electrons and the local 4f moments. The analysis suggests that the ordered phase may provide the first example of a half-metallic semimetal, and that the physics of EuB_6 should be described in terms of a two band Kondo lattice model with parallel (ferromagnetic) coupling of the conduction electrons and antiparallel (antiferromagnetic) coupling of the valence electrons to the local 4f moments.

PACS numbers: 75.30.Et,71.20.Eh,71.10.Fd,75.50.Cc

I. INTRODUCTION

Despite numerous experimental and theoretical studies, understanding of the electronic properties and magnetic coupling of EuB_6 still provides challenges. While having a simple crystal structure, consisting of a simple cubic lattice of Eu atoms with a B_6 octahedron located in the center of each cubic cell, nevertheless the transport and magnetic properties of this system are complex. EuB_6 orders ferromagnetically at 15.1 K, which is accompanied by a huge decrease of resistivity and a significant blue shift of the reflectivity plasma edge.[1] At 12.7 K another phase transition takes place, which is observed as a broad peak in the specific heat or an anomaly in the resistivity.[2] The origin of this transition is still unclear, with possible explanations including spin reorientation[3] or a long-wavelength modulation of the spin density.[4] Besides these properties, EuB_6 exhibits a rather sluggish increase of magnetization with decreasing temperature[5] and unusual pressure dependence of the Curie temperature with strong increase up to 70 kbar and a flat dependence at higher pressures.[6]

The LDA electronic structure of EuB_6 was previously investigated by Hasegawa and Yanase[7] and Massida et al.[8] Small overlap of conduction and valence bands was found resulting in Fermi surface pockets centered at the X point of the Brillouin zone. Isostructural CaB_6 and SrB_6 have similar bandstructures, which have seemed to be consistent with their observed transport properties[9] (although they are not understood in any detail). Recently CaB_6 has been studied with several variants of the GW method: the conventional pseudopotential GW,[10] and all-electron GW,[11] and a self-consistent GW method.[12] While there are differing results among these, the majority of them predict the opening of a gap of the order of 1 eV, making the LDA conclusions about the groundstate of divalent hexaborides questionable. Recent angle-resolved photoemission measurements[13,14] reported a bandgap in CaB_6, and only recently has it been demonstrated that synthesis from ultrapure boron[15] leads to transport properties that are characteristic of a semiconductor rather than a semimetal. For the paramagnetic phase of EuB_6, a bandgap was also observed,[13] below an occupied electron pocket at the X point that was interpreted as carriers resulting from (a high density of B) vacancies. Recently the transport properties have been interpreted in terms of a similar model.[16]

As usual in LDA-based band structure calculations of rare earth systems, the 4f states must be treated in a special way in order to insure their correct filling. In order to enforce the correct filling the 4f states were treated separately from the rest of the system in Ref. 8, neglecting any hybridization involving the f states and thus giving no insight into magnetic coupling mechanisms in EuB_6. Here we use the LDA+U method, which obtains the correct 4f state filling while keeping these 4f states in the same Hilbert space as the rest of the system, and so allows for mixing of 4f states with the valence states. The aim of the present work is to investigate the effective exchange interaction between the localized f moments and the band electrons. For this purpose we perform a detailed analysis of the orbital character and dispersion of the states close to the Fermi level. Based on this analysis we suggest an unusual two band Kondo lattice model to be the relevant picture for understanding the magnetic behavior of EuB_6.

II. COMPUTATIONAL DETAILS

The calculations were performed using the full-potential linearized augmented-plane-waves (FLAPW) method as implemented in the Wien2k code.[17] The LDA+U method was used with the double-counting scheme of Anisimov and collaborators.[18] The standard parametrization of the on-site Coulomb interaction involves two parameters U and J. However, since we are dealing with the Eu^{2+} f^7 ion, which has completely filled spin-up f shell and completely empty spin-down f shell, the role of J reduces to merely renormalizing the U value. Therefore we can set J=0 and quote just the U value.

All the presented calculations were performed with LDA exchange-correlation potential in the parameterization of Perdew and Wang.[19] The calculations were performed without spin-orbit coupling in the scalar relativistic approximation as implemented of Wien2k code.

The following computational parameters were used. The atomic radii were 2.7 and 1.5 Bohr for Eu and B respectively. The APW + lo basis set[20], with additional local orbitals for Eu 5s and 5p states, was characterized by plane-wave cut-o $R_{mt}K_{max} = 7$. We used 56 k-points in 1/48 irreducible wedge of the Brillouin zone. The numerical convergence of the total energy was better than 0.1 mRy. The internal parameter was relaxed so that the corresponding force was smaller than 1 mRy/a.u.

III. RESULTS AND ANALYSIS

A. Bulk properties

We have performed total energy vs. volume calculations in order to (i) determine the theoretical equilibrium volume and bulk modulus and (ii) investigate the influence of pressure on the band structure. For each value of lattice constant we have optimized the nearest-neighbor B-B distance (the only free internal parameter) using atomic forces. The calculated energy vs. volume curve is shown in Fig. 1. The inset shows the scaling of B-B distances with the lattice constant indicating that the bonds within B-octahedra are more rigid than the nearest-neighbor (inter-octahedra) B-B bond. The calculated equilibrium volume of 70.1 A^3 is about 96 % of the experimental value.[3] The calculated bulk modulus of 161 GPa is agrees very well with the experimental value.[21] The present results were obtained with U = 7 eV, however similar calculations performed for U = 6, 8, and 9 eV (without optimization of the internal parameter) showed that the bulk properties are insensitive to the value of U.

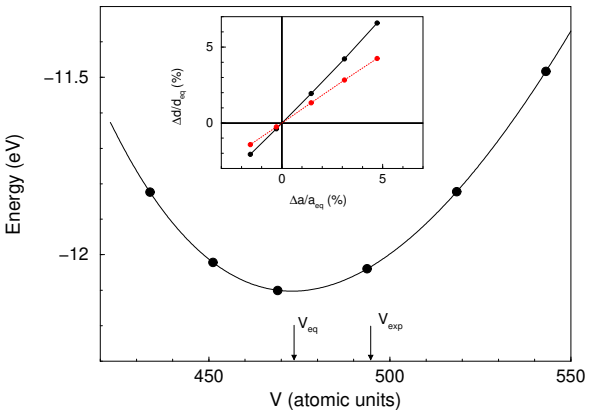

FIG. 1: The total energy vs. volume curve calculated with U = 7eV. In the inset the relative change of the nearest-neighbor (dotted) and intra-octahedron (solid) B–B distance as a function of relative change of the lattice constant.

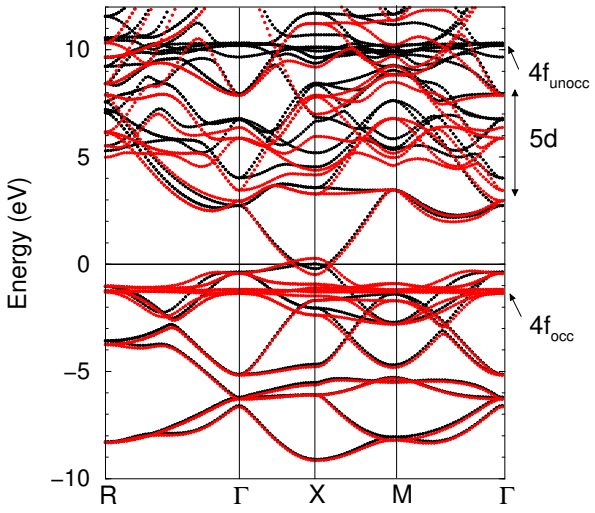

FIG. 2: Spin-polarized density band structure obtained with U = 7eV at the experimental lattice constant. The spin-up bands are marked red (brighter).

B. Bandstructure and exchange coupling

In Fig. 2 we show the spin-polarized bandstructure obtained at the experimental lattice constant with U = 7 eV. Taken literally, the bandstructure indicates a metallic ground-state with band overlap (negative gap) around X point in both spin channels. More importantly the overlap of majority (spin up) bands is strongly enhanced in comparison to minority (spin down) bands. The origin of the different band overlap is the opposite sign of the up/down exchange splitting induced in the conduction and valence band. While lowering of the energy of the spin-up conduction band with respect to the spin-down band points to parallel coupling of conduction electrons to the local f moments, the energy of the spin-up valence band is higher than that of the spin-down band indicating antiparallel coupling to the local f moments. In the following we investigate in detail origin of this particular effective exchange coupling. There are 6 symmetry related X points in the Brillouin zone of simple cubic structure. The following analysis is performed particularly for X = (0,0,1/2) and all references to spatial orientation the orbitals are with respect to this choice. Also, we do not distinguish between directions in real and k-space, which is not confusing for orthogonal unit cell.

The modulus of the wave-function corresponding to valence band maximum at the X point is shown in Fig. 3. In Fig. 4 we show the schematic plot of the same wave function in terms of B-p and Eu-f orbitals. Let us make several observations: (i) p-orbitals of B atoms at (1/2,1/2,z) do not contribute to this wavefunction while the other B atoms (which lie in the z= 1/2 plane) con-

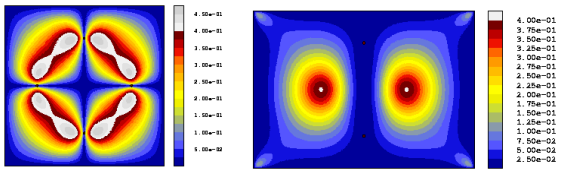

FIG. 3: Contour plot of the absolute value of the minority-spin valence band wavefunction at the X point. The right panel shows a cut through the boron plane (001) perpendicular to -X direction. The left panel shows a cut by (110) plane going through the center of the unit cell. Mixing with f state in corners of the plot is visible even for the minority spin. This feature is much stronger for the majority spin.

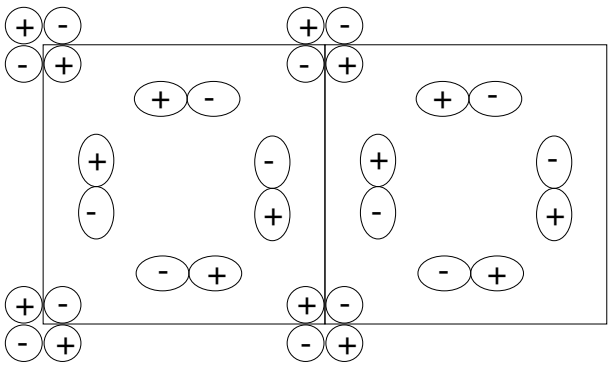

FIG. 4: Schematic plot of the valence band state at the X point showing the phases of participating orbitals. Two unit cells in X-M direction are shown.

tribute their p_x or p_y orbitals, (ii) hybridization between p orbitals in the neighboring unit cells (in X-M direction) is forbidden by symmetry at the X point, (iii) dispersion in the -X direction in enhanced by hybridization with Eu f orbital of xyz symmetry (note that this hybridization is allowed due to a phase shift of between adjacent Eu layers and thus is forbidden at point). Together points (ii) and (iii) explain the convex dispersion of the valence band with the top at the X point. The hybridization with Eu f also explains the antiparallel coupling of the valence electrons to the local f moments. The spin up valence orbital hybridizes strongly with the occupied f state localized close to the Fermi level and thus its energy is increased due to band repulsion. The hybridization shift (level repulsion) in the spin down channel is much weaker and of opposite sign, since the unoccupied f are localized high above the Fermi level due to the on-site Coulomb repulsion. As a result we obtain an effective antiferromagnetic exchange interaction of kinematic origin in the way described by the periodic Anderson model.[22]

Similar analysis is performed now for conduction band. By analyzing the orbital contributions to the conduction band we find that it contains a mixture of B-p and Eu-d states, where the d content decreases when going away from the X point and vanishes at the point. We show

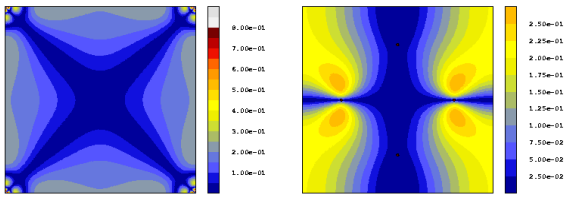

FIG. 5: Contour plot of the absolute value of the minority-spin conduction band wavefunction at the X point. The left panel shows a cut through the Eu plane (001) perpendicular to -X direction. The right panel shows a cut through the center of the unit cell by the (100) plane.

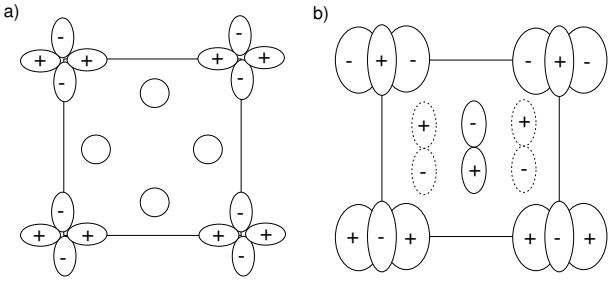

FIG. 6: Schematic plot of the conduction band state at the X point showing the phases of participating orbitals. The left panel shows the view along the -X direction. The right panel shows the view along the X-M direction.

the calculated modulus of the wave-function corresponding to the conduction band at the X point in Fig. 5 and the corresponding schematic plot in Fig. 6. We make following observations: (i) the only orbitals that contribute significantly are p_z orbitals localized on B atoms in the z= 1/2 plane and Eu $d_{x^2-y^2}$ orbitals, (ii) at the X point the p orbitals in the neighboring unit cells (in X-M direction) form a bonding orbital, which can hybridize with Eu $d_{x^2-y^2}$ orbital, going away in the X-M direction introduces a phase shift between p orbitals in neighboring cells a reduces hybridization with the d states, eventually at the M point the p orbitals form an antibonding combination and hybridization with d's is suppressed, (iii) looking along X- direction we find that the phase shift of at X point allows the p states to hybridize with Eu $d_{x^2-y^2}$ states while this mixing is forbidden at point. In conclusion the points (ii) and (iii) explain the concave dispersion of the conduction band with bottom at the X point. The conduction band originates from the B p band which mixes strongly with Eu $d_{x^2-y^2}$ band close to the X point. This picture is corroborated by the band-structure of the empty boron lattice (without Eu atoms) shown in Fig. 7, which contains a similar conduction band but with greatly reduced dispersion. The exchange interaction of the electrons in the conduction band with local f moments is of ferromagnetic f d intra-atomic origin. Both the reduced value of the exchange splitting

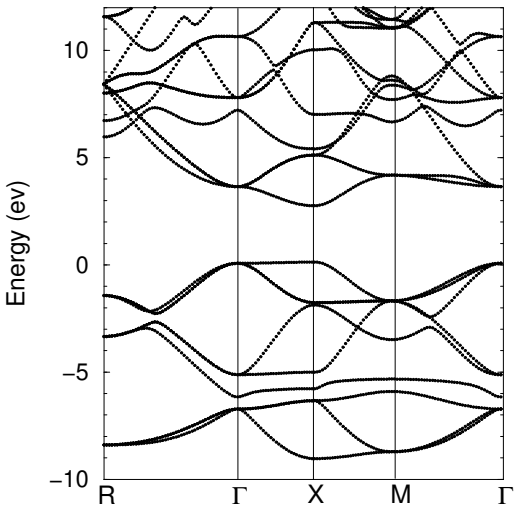

FIG. 7: The band structure of empty boron cage. The correct filling (2 additional electrons per octahedron) was achieved by virtual crystal approach.

as compared to higher lying d-bands and decrease of the exchange splitting when going away from X point are easily explained by variable content of the Eu d in the conduction band states as described in (ii) and (iii).

C. Role of Pressure and U

In the previous section we have shown that the mechanism of exchange with the local f moments is rather different for conduction and valence electrons. The conduction electrons are polarized through intra-atomic exchange interaction between the Eu d and f states. The strength of the interaction is determined mostly by the content of the d orbital in a particular wavefunction and is independent of the energy of f states. The polarization of valence electrons arises from different hybridization splitting in spin-up and spin-down channel. Since the hybridization is negligible in the minority channel, the strength of the effective exchange is determined by hybridization shift of the majority valence states. This shift is inversely proportional to the energy difference between the f and valence band. The position on the energy scale of the f states is therefore crucial for determining the strength of the effective exchange.

The position of the lower and upper 4f bands is determined by two factors within the LDA+U approach: (i) the center of gravity of the LDA f bands, (ii) the screened on-site Coulomb interaction U. The center of gravity of the f bands depends on charge transfer, but its LDA position suffers from well-known self-interaction error. The additional terms in the LDA+U hamiltonian enforce the splitting into lower and upper Hubbard band and in an approximate way correct for the self-interaction error in the lower band. To calculate the precise value of U, besides the fact that it is defined in a somewhat loose sense, is beyond the scope of this work. The typical U quoted for 4f electrons after accounting for screening is between 7 and 9 eV. In Fig. 8 we show the band overlap in the majority spin channel as a function of U from 6 to 9 eV. We point out that U around 7 eV yields the f bands approximately 1 eV below the Fermi level, which is the position deduced from optical experiments[23] and therefore we assume the results for this value to be most realistic.

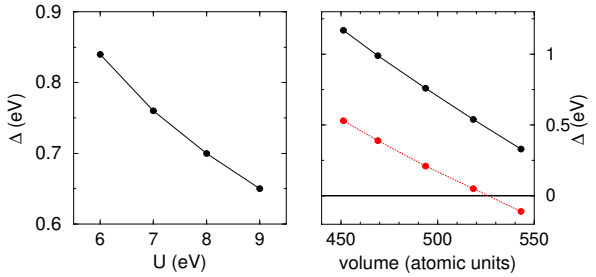

FIG. 8: The band overlap of the spin-up bands as a function of the parameter U evaluated at the experimental volume is shown in the left panel. The band overlap in the spin-up channel (upper curve) and spin-down channel (lower curve) as a function of unit cell volume evaluated at U = 7 eV.

The effect of applied pressure amounts to overall broadening of the bands and thus enhanced overlap of the conduction and valence bands at the X point. For a unit cell volume increase of about 10% a gap in the minority spin channel opens, while an appreciable overlap remains in the majority spin channel (see Fig. 8).

D. Model Hamiltonian

In the previous sections we have described the origin of dispersion and effective exchange coupling with local f moment in both valence and conduction bands. Based on the band structure we suggest the following model hamiltonian to provide a reasonable description of the low energy physics:

$$H = \sum_{k,} {}^{v}_{k} {}^{v\dagger}_{k} {}^{v}_{k} + {}^{c}_{k} {}^{c\dagger}_{k} {}^{c}_{k} \\ \frac{1}{L} \sum_{i,kk'} J^{v}_{i;kk'} S_i \; {}^{v\dagger}_{k} \; {}^{v}_{k'} + \\ J^{c}_{i;kk'} S_i \; {}^{v\dagger}_{k} \; {}^{c}_{k'} \; ; \qquad (1)$$

where operators v_k and c_k correspond to valence and conduction bands respectively, S_i is a total spin operator of the local f moments and L is the number of unit cells in the normalization volume.

Obtaining parameters of the model hamiltonian from the bandstructure is not a straightforward task, in particular the choice of the reference non-interacting state is

tricky. It was shown by Schiller and Nolting[24] and further discussed by Muller and Nolting[25] that in case of k-independent exchange parameter J, the majority-spin band is rigidly shifted with respect to its non-interacting counterpart, while the minority-spin band is modified beyond the rigid shift due to interaction with the local moments. The situation in EuB_6 is more complicated since, as discussed below in detail, the exchange parameter is strongly k-dependent for purely chemical reasons (hybridization). It is therefore not possible to distinguish unambiguously the deviation of the exchange splitting (k) from a rigid band shift arising from the correlation effects in the minority-spin band from that originating in the 'chemical' k-dependence of the exchange parameter J. Since the k-dependence of the exchange splitting (k) along the X- and X-M directions is very pronounced and can be qualitatively understood in terms of k-dependent exchange parameter J we neglect the correlation effects in the minority spin channel.

The non-interacting dispersion relations $^{v}_{k}$ and $^{c}_{k}$ obtained from the bandstructure (Fig. 2) are considered separately. The interaction of the conduction electrons with the local moments is dominated by the f d intra atomic exchange depending only on the d content in a particular conduction state. The 'non-interacting' conduction band is then approximated by an average of the spin-up and spin-down bands. Since the hybridization in the majority band is the source of the exchange splitting in the valence band, the 'non-interacting' valence band is well approximated by the spin-down band. The Fermi level is located close to the top, resp. bottom, of the valence, resp. conduction, band and so the low energy bandstructure can be parametrized by anisotropic effective masses and the band overlap. The effective mass tensor for an ellipsoid of revolution is characterized by only two independent parameters $_{?}$ and $_{k}$ corresponding to X-M and X- dispersion respectively. The effective masses obtained by parabolic fit from the bandstructure (Fig. 2) are $^{c}_{?} = 0.23$, $^{c}_{k} = 0.47$, $^{v}_{?} = 0.25$, and $^{v}_{k} = 2.2$. The band overlap of the 'non-interacting' bands at X point is 0.34 eV. We point out that using the spin-up conduction band as a non-interacting reference (rigidly shifted) does not lead to significant modification of the effective masses.

Since the mechanisms of effective exchange with local moments are different we have to discuss determination of the corresponding coupling constants $J_{i;kk^0}$ separately. The kk^0 dependent coupling constants can not be determined directly from the bandstructure and additional assumptions must be made. We start with the conduction band.

We mentioned earlier that the conduction band coupling to the local moment is mostly due to intra-atomic f d exchange described by

$$H_{df} = \sum_{i;} J \; S_i \; \hat{d}^{y}_{} \; d_i \; ; \qquad (2)$$

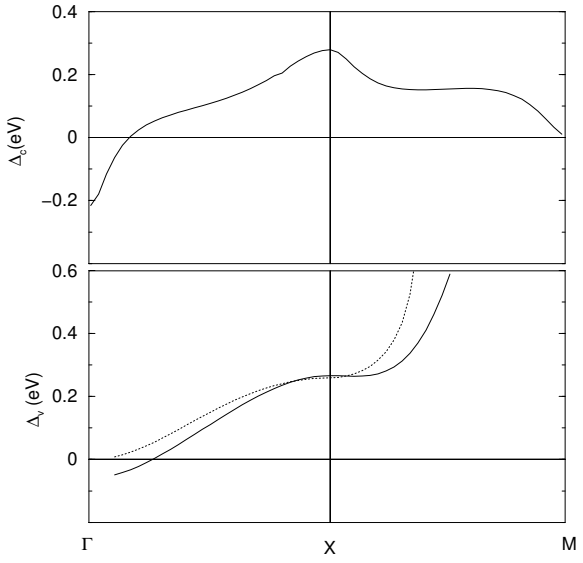

FIG. 9: The k-dependent exchange splitting: splitting of the conduction band is shown in the upper panel, the splitting of the valence band is shown in the bottom panel. The exchange splitting calculated with the tight-binding expression for $V_{fp} = 24$ meV is marked with the dotted line.

which leads to

$$J_{i;kk^0} = J e^{i(k \; k^{\;0}) R_i} : \qquad (3)$$

However, the conduction band is not a pure d-band, but contains a mixture of d and p orbitals $c_k = (k) d_k + (k) p_k$. Treating H_{df} as a first order perturbation leads to an effective coupling of the conduction of the form

$$J^{c}_{i;kk^0} = J e^{i(k \; k^{\;0}) R_i} \; (k) \; (k^{\;0}) : \qquad (4)$$

Here can be chosen at convenience as real and positive. Finally we make connection to the band structure by observation that the k-dependent exchange splitting of the conduction band is given by

$$^{c}(k) = ^{c}_{k\#} \; ^{c}_{k"} = 2JS \; ^{2}(k) : \qquad (5)$$

Finally putting (4) and (5) together we obtain

$$2S J^{c}_{i;kk^0} = e^{i(k \; k^{\;0}) R_i} \sqrt{^{c}(k) \; ^{c}(k^0)} : \qquad (6)$$

The k-dependent exchange splitting of the conduction band is shown in Fig. 9. Vanishing of the exchange splitting when the and M points are approached can be understood in terms of simple nearest neighbor (NN) hopping picture. The k-dependent hybridization between p and d bands vanishes at and M, and thus the valence states have a pure p character at these points. The p d NN hopping in the conduction band has the same symmetry as the p f hopping in the valence band leading to the same k-dependence of the hybridization (9) and (10) discussed below.

For the valence band the effective exchange coupling arises by Schrieffer–Wolff transformation[26] from Anderson lattice hamiltonian with the f – p hopping term

$$H_{pf} = \sum_{i,k,\sigma} V_{ik} f_i^{\dagger} v_{k\sigma} + h.c. \qquad (7)$$

The corresponding exchange parameter for states close to the Fermi level (i.e. far enough from the f band) is given by

$$J^{v}_{i,kk'} = \frac{1}{2} V_{ki} V_{ik'} \left(\frac{1}{\epsilon_k - \epsilon_f} + \frac{1}{\epsilon_{k'} - \epsilon_f} \right) \left(\frac{1}{\epsilon_k - \epsilon_f - U} + \frac{1}{\epsilon_{k'} - \epsilon_f - U} \right), \qquad (8)$$

where ϵ_f is the energy of the occupied f states and $\epsilon_f + U$ is the energy of the unoccupied f states. As in the case of the conduction band we have to make additional assumption in order to extract information about $J^{v}_{i,kk'}$ from the bandstructure. The natural assumption in terms of the local orbitals is to expect non-zero hopping V_{fp} only between the nearest neighbor p and f (xyz) orbitals (see Fig. 4). Note that the sign of V_{fp}, given by symmetry of the orbitals, is different for different pairs of orbitals (each p orbital has 8 NN f orbitals). In particular, pairs connected by a vector $(m, n, 1/2)$ have the same sign, which is opposite to the sign for pairs connected by $(m, n, -1/2)$ $(m, n = -1/2)$. Now we can write down the matrix element V_{ki} as

$$V_{ik} = 2\frac{V_{fp}}{L}\sqrt{\quad} e^{-i k R_i} F(k), \qquad (9)$$

where

$$F(k) = \sin\frac{ak_x}{2}\sin\frac{ak_y}{2}\sin\frac{ak_z}{2} + \sin\frac{ak_x}{2}\sin\frac{ak_y}{2}\sin\frac{-ak_z}{2} + \sin\frac{ak_x}{2}\sin\frac{-ak_y}{2}\sin\frac{ak_z}{2} + \sin\frac{-ak_x}{2}\sin\frac{ak_y}{2}\sin\frac{ak_z}{2}. \qquad (10)$$

Providing we know the value of the hopping parameter V_{fp} the coupling $J^{v}_{i,kk'}$ can be calculated by feeding the above expression and the known dispersion relation into equation (8). In order to obtain the parameter V_{fp} we express the exchange splitting of the valence band as

$$\Delta^{v}(k) = \epsilon^{v}_{k\uparrow} - \epsilon^{v}_{k\downarrow} = 8 S V_{fp}^2 F(k)^2 \left[\frac{1}{\epsilon_k - \epsilon_f} - \frac{1}{\epsilon_k - \epsilon_f - U} \right], \qquad (11)$$

and use the fact that along the Γ–X direction $F(k) = 4\sin(ak_z/2)$, while along the X–M direction $F(k) = 4\cos(ak_x/2)$. The exchange splitting of 0.26 eV and $\epsilon_k - \epsilon_f \approx 1$ eV at the X point yield $V_{fp} = 24$ meV. In Fig. 9 we show the k-dependent exchange splitting together with the expected k-dependence. For the X–M direction we show only the region close to the Fermi level. The reason is that close to the crossing of the non-interacting band with the f level the exchange splitting $\Delta(k)$ is not well defined.

E. Mean field results

Here we want to illustrate the potential usefulness of the suggested hamiltonian by investigating some of its – nite temperature properties in mean field approximation. Due to the three dimensionality and the large moment, mean field should be realistic in many respects. A similar approach was taken by Korenblit[4] without providing detailed results. We focus on the role of the exchange enhanced band overlap and its consequences. In the mean field approximation the hamiltonian (1) reduces to

$$H_{MF} = \sum_{k,\sigma} \epsilon^{v}_{k\sigma} v^{\dagger}_{k\sigma} v_{k\sigma} + \epsilon^{c}_{k\sigma} c^{\dagger}_{k\sigma} c_{k\sigma} - h \sum_i S^z_i; \qquad (12)$$

where the spin-dependent dispersion relations are given by $\epsilon^{a}_{k\sigma} = \epsilon^{a}_{k} - J^a \langle S^z \rangle \sigma$ and $h = \sum_a J^a (n^a_{\uparrow} - n^a_{\downarrow})$ is an effective self-consistent magnetic field, with $a = v, c$ and $\sigma = \pm 1$. The quantities $n^a_{\uparrow}, n^a_{\downarrow}$ are the occupations of the bands. Going to the hole picture of the valence band and using the charge neutrality condition to determine the Fermi level we obtain the following set of equations

$$\sum_k n_c(S^z) - n_v(S^z) = 0 \qquad (13)$$

$$h = \sum_k J^c n_c(S^z) - J^v n_v(S^z) \qquad (14)$$

$$S^z = B_{7/2}\left(\frac{h}{k_B T} \right); \qquad (15)$$

where $B_{7/2}(x)$ is the Brillouin function for $S = 7/2$.

We have solved the mean field equations using the effective masses listed above. To make the analysis as simple as possible we approximate the coupling parameters J with a single k-independent constant (with opposite sign for the valence and conduction bands). To assess sensitivity of the model to the choice of J, we have used two values: (i) $|J| = 0.04$ eV corresponding to the X point exchange splitting of 0.28 eV (see Fig. 2) and (ii) $|J| = 0.10$ eV used by Korenblit.[4] The calculated ordered moment vs. temperature $S_z(T)$ curves are shown in Fig. 8. There are two distinct regimes.

(i) For band overlap $\Delta < 0$ (i.e. bandgap of $|\Delta|$) there is a minimum ordered moment S_{min} necessary to establish the overlap of spin-up bands. Below this value the magnetization cannot be self-stabilized since the corresponding effective field h is zero. Solution of equation (15) can be visualized as the intersection, on the interval (0,7/2], of the right-hand side $s = B_{7/2}$ as a function of S^z, given by (14), and the straight line $s = S^z$ of the left-hand side. The right-hand side is zero for

$S < S_{min}$ and, from definition of $B_{7/2}(x)$, less or equal to 7/2. This means that curve representing the right-hand side must cross the line representing the left-hand side an even number of times since it is continuous and its initial and final points are in the same half-plane determined by the left-hand side. Therefore there must be an even number of non-zero solutions of (15) for < 0 and a given temperature. In our case it means either zero or two solutions.

In order to identify, in the two solution case, the solution with lower free energy we approximate the total free energy by the sum of the free energy of non-interacting valence and conduction electrons evaluated with the self-consistent value of the effective field h and the free energy of non-interacting local moments in the effective field h at a given temperature. In all cases we find that the solution with larger ordered moment corresponds to the lower free energy.

The hamiltonian (1) preserves separately the number of electrons in valence and conduction bands. If those bands are completely filled or empty in the non-interacting ground state, which is degenerate with respect to orientation of the local moments, there is no effective coupling between the local moments since the degenerate grounstate manifold is disconnected from the excited states. On the other hand when a minimum net magnetization already exists a band overlap is induced and a magnetic groundstate can be found as described by the mean field equations. There is no continuous connection between the non-magnetic and magnetic states and therefore we conclude that the transition is of the first order.

(ii) For > 0 one solution exists in most of the studied cases, with the ordering temperature increasing as increases. The magnetization versus temperature behavior deviates from the standard Weiss curve, which is obtained for linear dependence of the effective field h on S_z. In a narrow range of close to zero three solutions may exist, providing yet another phase transition below the magnetic{nonmagnetic one. We do not make any conclusions about the order of the phase transition in this parameter range. In the insets of Fig. 8 we show the ordering temperatures as a function of band overlaps. The difference between the ordering temperatures obtained with different coupling constants J indicates a strongly non-linear T_C vs. J dependence. (Note that if the band shifts due to the ordering of the local moments are very small, $T_C \propto J^2$ Ref. 4).

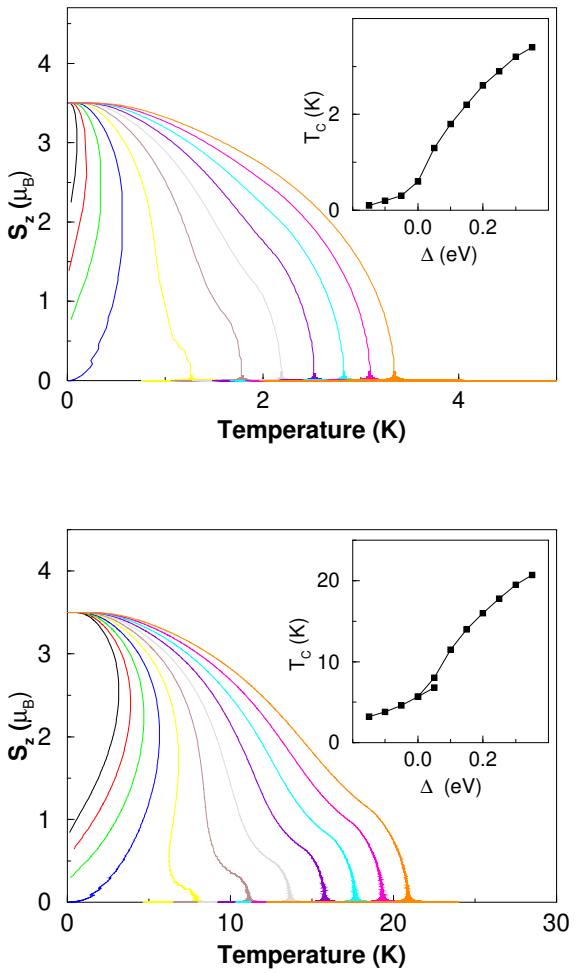

FIG. 10: Ordered spin moment vs. temperature evaluated from the mean-field model for various values of the band overlap. The upper and lower panel correspond to J = 0.04 and 0.1 eV respectively. The magnetization curves, ordered from the left to the right, correspond to band overlaps from -0.15 eV (bandgap) to 0.35 eV (with a step of 0.05 eV). The ordering temperatures as a function of the band overlaps are shown in the insets. The lower T_C for J = 0.1 eV and = 0.05eV correcpond to the second phase transition.

IV. DISCUSSION

One of the controversial questions concerning divalent alkaline earth hexaborides is whether the groundstate is insulating or metallic at stoichiometry. The experimental as well as theoretical evidence is controversial. Recent LDA calculations by Massidda et al[8] neglecting the magnetic order yield a metallic band structure for EuB_6 similar to that of CaB_6 or SrB_6 with a small band overlap of about 0.3 eV. The selfconsistent GW calculation[12] finds CaB_6 to be a semiconductor with a band gap of the order of 1 eV, as does the more conventional pseudopotential GW calculation.[10] The GW method is known to provide good bandgaps for many semiconductors where the LDA gaps are strongly underestimated or even vanishing. The effect of GW self-energy corrections on the EuB_6 bandstructure is expected to be similar, thus reducing the band overlap and possibly opening a band gap by shifting the conduction band upwards.

An important difference between EuB_6 and CaB_6 is the presence of 4f orbitals. We have shown that the exchange interaction with the band electrons is opposite in sign for the valence and conduction bands, so magnetic order

can significantly increase the overlap of the majority spin band while it has opposite effect for the minority spin. Although the effective exchange with the valence band depends on the position of the 4f states and thus varies somewhat with the parameter U, general experience with rare earth systems as well as optical measurements on EuB_6[23] indicate that U of 7 eV (placing the Eu 4f 1 eV below the Fermi level) is realistic.

Based on these arguments it is plausible that the realistic ground state picture of stochiometric EuB_6 is that of a half metallic semimetal. This unprecedented band structure would result from a ferromagnetic GW calculation in which the band shifts (relative to the static LDA+U) are large open a gap in the minority spin channel, but not so large as to open a gap in the majority spin channel. Such a scenario has some experimental support. de Haas–van Alphen data provide clear indication of Fermi surfaces, but only two pockets are seen.[27,28] This number of sheets is contrary to the expected four pockets suggested by LDA (and LDA+U) band structure, but two sheets are exactly what is expected of a half metallic semimetal.

The observed behavior of the resistivity is also consistent with such a picture. In the magnetically ordered state, metallic conduction takes place in the majority spin channel. Just above the magnetic ordering temperature the system can be viewed as consisting of disordered magnetic domains (due to short range ferromagnetic correlations), and the increase of resistivity upon disordering is due to mismatch of the conducting spin channels between these domains (like the "intergrain tunneling mechanism" of giant magnetoresistance materials; see e.g. Ref. 29). Increasing the temperature further leads to breakdown of the short range order, the paramagnetic bandstructure becomes increasingly appropriate, and the inter-domain magnetoresistance effect disappears, as observed.

Angle-resolved photoemission data[13] do not seem to fit well into this picture, but further photoemission studies in the ordered phase, and identifying the position and influence of the f states, seems to be necessary to clarify several remaining questions. The very large number of electron carriers that the photoemission data, if assumed to be representative of the bulk, does not fit so well with data that suggest rather clean single crystals. If the carriers are due to unbalanced surface charge, then the observed bands are not representative of the bulk. Finally, the broken inter-octahedron B–B bonds should give rise to surface states (or bands), and the implication of the photoemission data will never be unambiguous until the surface electronic structure is identified and understood.

Finally we discuss briefly our mean field treatment of the two band Kondo lattice model hamiltonian. We expect that the least reliable quantity obtained from the electronic structure calculation is the band overlap, and we have treated it as a parameter in the mean field study. The two band hamiltonian even in mean field approximation leads to a strongly temperature dependent coupling between the local moments, which is reflected by unusual magnetization dependences distinct from the canonical behavior of the Heisenberg hamiltonian in mean field. The solutions for small positive band overlap exhibit a slow approach to saturation as observed,[5] as well as an increase of the ordering temperature with pressure,[6] i.e. with increasing band overlap. The ordering temperatures obtained with the ab initio value of the exchange parameter J are, however, too low compared to experiment. We mention several possible reasons for this discrepancy. First, we have completely neglected the k-dependence of the exchange parameter J. Second, equation (8) shows that the value of J^v is quite sensitive to the position of the occupied 4f levels, which we know only approximately. And finally, some mechanisms of effective exchange between the local moments arising from the Anderson model are lost when transformed to the Kondo model (e.g. superexchange). These mechanisms might be of importance in the < 0 case leading to removal of the first order transition. The mean field study does serve to demonstrate the potential usefulness of the two-band hamiltonian and to stimulate further studies by more advanced techniques, such as the Green's function approach of Nolting et al.[30]

V. CONCLUSIONS

Using the LDA+U approach we have shown that treating the Eu 4f states within the same framework as the rest of the itinerant electrons has important consequences. In particular it leads to Kondo coupling between local moments and valence electrons, but anti-Kondo coupling to conduction electrons. We have identified and described in detail the origin of this coupling as well as the origin of the k-dependence of the anti-Kondo (ferromagnetic) coupling to the conduction band. Based on our electronic structure analysis we suggest the description of EuB_6 in terms of two band Kondo/anti-Kondo lattice model, and shown that a half metallic semimetal results at the mean field level of description. We have obtained the parameters of the corresponding hamiltonian, which will allow more extensive material-specific treatments in the future, and demonstrated the effects on magnetic ordering arising from an exchange controlled band overlap. The picture we present seems consistent with observed Fermi surfaces and transport properties.

VI. ACKNOWLEDGEMENT

We highly appreciate stimulating discussions with Wei Ku. This work was supported by Czech-USA Project No. KONTAKT ME547, by the NATO/NSF Grant No. DGE-0209264, and by NSF Grant No. DMR-0114818.

[1] L. Degiorgi, E. Felder, H. R. Ott, J. L. Sarrao, and Z. Fisk, Phys. Rev. Lett. 79, 5134 (1997).
[2] S. Sullow, I. Prasad, M. C. Aronson, S. Bogdanovich, J. L. Sarrao, and Z. Fisk, Phys. Rev. B 62, 11626 (2000).
[3] S. Sullow, I. Prasad, M. C. Aronson, J. L. Sarrao, Z. Fisk, D. Hristova, A. H. Lacerda, M. F. Hundley, A. Vigliante, and D. Gibbs, Phys. Rev. B 57, 5860 (1998).
[4] I. Y. Korenblit, Phys. Rev. B 64, 100405 (2001).
[5] W. Henggeler, H.-R. Ott, D. P. Young, and Z. Fisk, Solid State Commun. 108, 929 (1998).
[6] J. C. Cooley, M. C. Aronson, J. L. Sarrao, and Z. Fisk, Phys. Rev. B 56, 14541 (1997).
[7] A. Hasegawa and A. Yanase, J. Phys. C 12, 5431 (1979).
[8] S. Massidda, A. Continenza, T. M. de Pascale, and R. Monnier, Z. Phys. B 102, 83 (1997).
[9] C. O. Rodriguez, R. Weht, and W. E. Pickett, Phys. Rev. Lett. 84, 3903 (2000).
[10] H. J. Tromp, P. van Gelderen, P. J. Kelly, G. Brocks, and P. A. Bobbert, Phys. Rev. Lett. 87, 016401 (2001).
[11] H. Kino, F. Aryasetiawan, K. Terakura, and T. Miyake, Phys. Rev. B 66, 121103 (2002).
[12] W. Ku, private communication.
[13] J. D. Denlinger, J. A. Clark, J. W. Allen, G.-H. Gweon, D. M. Poirier, C. G. Olson, J. L. Sarrao, A. D. Bianchi, and Z. Fisk, Phys. Rev. Lett. 89, 157601 (2002).
[14] S. Souma, H. Komatsu, T. Takahashi, R. Kaji, T. Sasaki, Y. Yokoo, and J. Akimitsu, Phys. Rev. Lett. 90, 027202 (2003).
[15] J.-S. Rhyee, B. H. Oh, B. K. Cho, M. H. Jung, H. C. Kim, Y. K. Yoon, J. H. Kim, and T. Ekino, cond-mat/0310068, (2003).
[16] G. A.. Wigger, R. Monnier, H. R. Ott, D. P. Young, and Z. Fisk, cond-mat/0309412, (2003).
[17] P. Blaha, K. Schwarz, G. K. H. Madsen, D. Kvasnicka, and J. Luitz, WIEN2k, An Augmented Plane Wave + Local Orbitals Program for Calculating Crystal Properties (Karlheinz Schwarz, Techn. Universitat Wien, Wien, 2001), ISBN 3-9501031-1-2.
[18] V. I. Anisimov, I. V. Solovyev, M. A. Korotin, M. T. Czyzyk, and G. A. Sawatzky, Phys. Rev. B 48, 16929 (1993).
[19] J. P. Perdew and Y. Wang, Phys. Rev. B 45, 13244 (1992).
[20] E. Sjostedt, L. Nordstrom, and D. J. Singh, Solid State Commun. 114, 15 (2000).
[21] S. Zherlitsyn, B. Wolf, B. Luthi, P. Hinze, E. Uhrig, W. Assmus, H. R. Ott, D. P. Young, and Z. Fisk, Eur. Phys. J B 22, 327 (2001).
[22] P. Fazekas, Lecture Notes on Electron Correlation and Magnetism (World Scientific, Singapore, 1999), ISBN 981-02-2474-5.
[23] S. Broderick, L. Degiorgi, H. R. Ott, J. L. Sarrao, and Z. Fisk, Eur. Phys. J. B 33, 47 (2003).
[24] R. Schiller and W. Nolting, Solid State Commun. 118, 173 (2001).
[25] W. Muller and W. Nolting, Phys. Rev. B 66, 085205 (2002).
[26] J. R. Schrieffer and P. A. Wolff, Phys. Rev. 149, 491 (1966).
[27] R. G. Goodrich, N. Harrison, J. J. Vuillemin, A. Teklu, D. W. Hall, Z. Fisk, D. Young, and J. Sarrao, Phys. Rev. B 58, 14896 (1998).
[28] M. C. Aronson, J. L. Sarrao, Z. Fisk, M. Whitton, and B. L. Brandt, Phys. Rev. B 59, 4720 (1999).
[29] H. Y. Hwang and C.-W. Cheong, Science 278, 1607 (1997).
[30] W. Nolting, S. Rex, and S. M. Jaya, J. Phys.: Condens. Matter 9, 1301 (1997).